

Natural Observers with Parameter Adaptation and Applications to Speed Sensorless DC Servo and Induction Motors

S. R. Bowes, *Fellow, IEEE*, A. Sevinç and D. Holliday

Abstract A simple observer design technique with parameter adaptation is proposed for bounded-input bounded-output non-linear systems. In this technique, no feedback is used in the observer but parameter estimations are considered as if they are observer inputs. The proposed technique is successfully applied to speed sensorless dc servomotors and speed sensorless induction motors with load torque adaptation schemes. The observer is robust to noise and parameter uncertainty. Excellent experimental and simulation results have been obtained.

I. INTRODUCTION

To date, a number of adaptive observer design techniques have been proposed for control systems [1-15]. However, none of these methods are easy to apply to a wide range of non-linear systems. These proposed methods are used either for a specific non-linear system or are very complicated to apply. In general, these observers have distinctly different structures from the actual plant. Consider the plant represented by (1)

$$\left. \begin{aligned} \dot{\mathbf{x}} &= \mathbf{f}(\mathbf{x}, \boldsymbol{\theta}) + \mathbf{B}\mathbf{u} \\ \mathbf{y} &= \mathbf{h}(\mathbf{x}) \end{aligned} \right\} \quad (1)$$

where \mathbf{x} , \mathbf{u} and \mathbf{y} are system state, input and output vectors respectively, $\boldsymbol{\theta}$ is the parameter vector to be estimated, \mathbf{f} and \mathbf{h} are non-linear system functions and \mathbf{B} is an input matrix. Based upon (1), the structure of conventional observers (adaptive or non-adaptive) is usually as shown in Figure 1. The adaptation block, which is shown within the broken lines, is optional. As can be seen, the number of inputs to the observer is different to the number of

inputs to the plant since the observer uses output feedback. This structural difference imposes serious restrictions on the selection of the observer gain matrix, \mathbf{L} , and on the initial error [1-13] for stability of the observer even when the actual system is stable. These restrictions are subject to complicated mathematical rules for non-linear systems [1-13]. If an adaptation algorithm is also applied, the restrictions become much more complicated and in some cases may be impossible to determine.

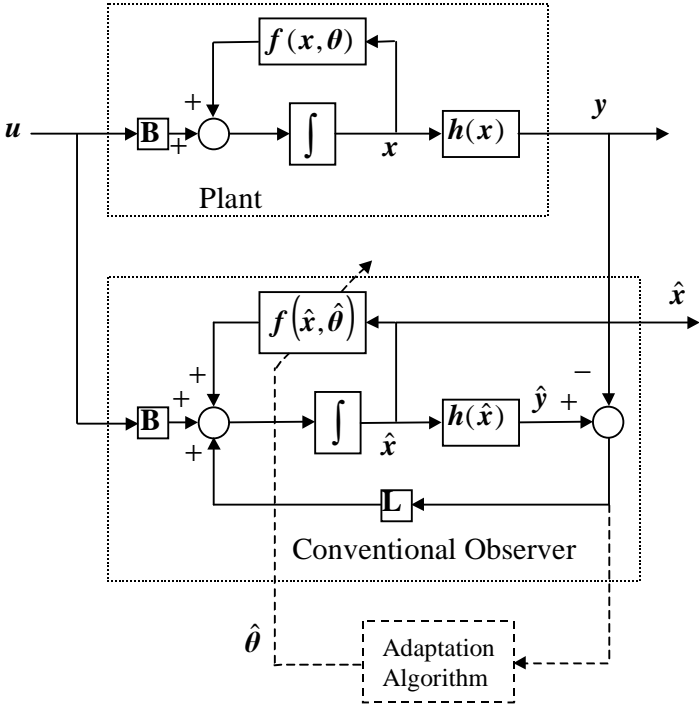


Figure 1: Conventional observer with an optional parameter adaptation block.

An additional problem with conventional observers is noise sensitivity [1-13]. The output measurement, y , is integrated just once in the calculation of \hat{x} (at least for some components of \hat{x}) and therefore the observer may not filter the measurement noise sufficiently [1-13].

For the reasons outlined previously, only a limited number of adaptive observer design techniques have been successfully applied to speed sensorless induction motors. The most promising ones are the Extended Kalman Filter (EKF) [1-3], the Extended Luenberger Observer (ELO) [4-6], Model Reference Adaptive System (MRAS) applications [7-10] and Kubota's adaptive observer [11-13]. However, many of these techniques are either too complicated or too time-consuming for real-time applications, particularly for variable operating conditions [1-13].

In this paper a simple technique, called the *natural observer*, with parameter adaptation is proposed to address the aforementioned problems. The proposed technique is simple to implement and is applicable to most bounded-input bounded-output stable systems. Additionally, very accurate estimations are obtained even with very noisy measurements. This paper presents application of the natural observer, with a load torque adaptation scheme, to a speed sensorless dc servo and to induction motor control.

II. THE NATURAL OBSERVER CONCEPT

The proposed observer, shown in Figure 2 for system (1), is in exactly the same form as the actual system model and has no external feedback, hence its dynamic behaviour is the same as the natural behaviour of the actual system. Therefore it is called a *natural observer*. Because the actual system is assumed to be bounded-input bounded-output stable, such an observer will also be bounded-input bounded-output stable. The basic principle for achieving convergence with this observer is to control the observer by means of the estimated parameters as if they are inputs. Whilst the parameter adaptation is optional for conventional observers, it is essential for natural observers. The most important difference between natural observers and conventional observers is that natural observers do not use feedback directly, the feedback being used only in the adaptation algorithm.

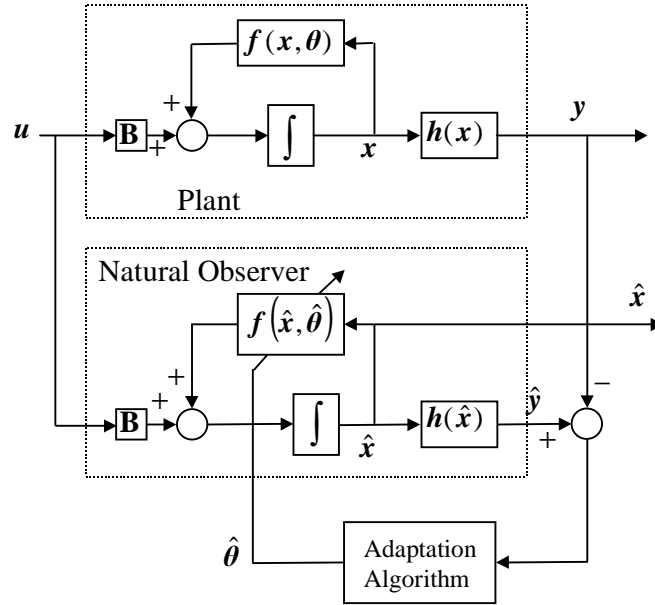


Figure 2: Block diagram of a natural observer with adaptation.

To control the observer with parameter adaptation, PID, PI or just integral schemes can be used so that suitably defined errors between the actual system and the observer approach zero. In order to keep the observer states bounded the parameter estimations are limited within predetermined ranges. Then, the bounded-input bounded-output stability guarantees the boundedness of the observer states in the majority of cases for specified ranges of parameter estimations. Suitable limits for the estimated parameters can be found from trial and error methods using simulation techniques. Furthermore, limiting the rates of the parameter estimations ensures smoother response. Another important advantage of the natural observer structure is that whilst conventional observers can yield large error peaks during transient operation making the control difficult, the natural observer's transient error remains relatively small as a result of its natural structure and the adaptive parameter estimation.

The natural observer design is not restricted to systems in the form defined by (1), which has been used to more clearly highlight the differences between the observers of Figures 1 and 2. For example, even for systems in the more general form (2)

$$\left. \begin{aligned} \dot{\mathbf{x}} &= \mathbf{f}(\mathbf{x}, \mathbf{u}, \boldsymbol{\theta}) \\ \mathbf{y} &= \mathbf{h}(\mathbf{x}) \end{aligned} \right\} \quad (2)$$

a natural observer may still be designed. Because there is a wide range of possible nonlinearities, presentation of the application of the natural observer in a general form is difficult. Therefore, the following explanation is based on a speed sensorless dc servomotor and a speed sensorless induction motor.

III. THE NATURAL OBSERVER APPLICATIONS

A. Speed Sensorless DC Servomotor

Consider a second order dc servo motor model

$$\begin{bmatrix} \dot{\omega}_r \\ \dot{i}_a \end{bmatrix} = \begin{bmatrix} -f_d/J & K_t/J \\ -K_b/L_a & -R_a/L_a \end{bmatrix} \begin{bmatrix} \omega_r \\ i_a \end{bmatrix} + \begin{bmatrix} -T_L/J \\ 0 \end{bmatrix} + \begin{bmatrix} 0 \\ 1/L_a \end{bmatrix} v_a \quad (3)$$

where ω_r , i_a and v_a are rotor speed, armature current and armature voltage respectively, T_L is load torque, R_a and L_a are armature resistance and inductance, K_b and K_t are the back emf and torque constants, and f_d and J are friction constant and inertia respectively. Since speed sensorless operation is assumed, ω_r and T_L are assumed to be inaccessible and i_a is assumed as the output.

A natural observer with load torque adaptation can be designed simply as

$$\begin{bmatrix} \dot{\hat{\omega}}_r \\ \dot{\hat{i}}_a \end{bmatrix} = \begin{bmatrix} -f_d/J & K_t/J \\ -K_b/L_a & -R_a/L_a \end{bmatrix} \begin{bmatrix} \hat{\omega}_r \\ \hat{i}_a \end{bmatrix} + \begin{bmatrix} -\hat{T}_L/J \\ 0 \end{bmatrix} + \begin{bmatrix} 0 \\ 1/L_a \end{bmatrix} v_a \quad (4)$$

where $\hat{\omega}_r$, \hat{i}_a and \hat{T}_L are estimated speed, armature current and load torque respectively. This observer has the natural characteristics of the dc servomotor, such as bounded-input bounded-output stability, provided that \hat{T}_L is within certain limits. Under the same input voltage and load torque, both (3) and (4) approach the same states regardless of the initial conditions even though there is no output feedback in (4). Therefore, convergence of the natural observer can be achieved with an appropriate load torque adaptation. Based on the fact that the greater the load torque the greater the armature current, a PI or just integral control scheme using the armature current error can be designed to estimate the load torque. To ensure the bounded-input bounded-output stability of the natural observer, \hat{T}_L is limited within a range defined by lower and upper limits T_{\min} and T_{\max} :

$$\dot{\hat{T}}_L = \mu(\hat{i}_a - i_a) \quad \text{limiting} \quad \hat{T}_L \in [T_{\min}, T_{\max}] \quad (5)$$

where $\mu < 0$ since $(\hat{i}_a - i_a) > 0$ implies $\dot{\hat{T}}_L < 0$. As a result, the convergence of the natural observer (4) is achieved with the load torque adaptation scheme (5).

(4) and (5) do not require a specific control scheme. Applying a PID control with suitable PID gains, K_P , K_I and K_D ,

$$v_a = K_D \frac{d}{dt}(\omega_{ref} - \omega_r) + K_P(\omega_{ref} - \omega_r) + \int K_I(\omega_{ref} - \omega_r) dt \quad (6)$$

where ω_{ref} is the reference speed, which is usually piecewise constant, desired eigenvalues of the third order error dynamics can be obtained since the system is second order linear time-invariant, disregarding the term T_L/J which is also assumed piecewise constant and disappears in the third order error differential equation. Substituting $\dot{\omega}_r$ from (3), omitting

$\dot{\omega}_{ref}$ and T_L/J , which can be regarded as part of the integral constant, and using the observer states, \hat{i}_a and $\hat{\omega}_r$ instead of i_a and ω_r , (6) becomes

$$v_a = -K_D \frac{K_t}{J} \hat{i}_a + K_D \frac{f_d}{J} \hat{\omega}_r + K_P (\omega_{ref} - \hat{\omega}_r) + \int K_I (\omega_{ref} - \hat{\omega}_r) dt \quad (7)$$

(4), (5) and (7) construct an observer based adaptive control scheme for the servo motor, (3). A suitable gain, μ , and torque limits T_{min} and T_{max} are found from simulation.

This adaptive observer is very simple to apply and yields good results as will be seen in Section IV.

B. Speed Sensorless Induction Motor

An observer in exactly the same form as the actual induction motor model without any feedback has the natural characteristics of the actual motor, *i.e.* under the same conditions of load torque and input voltage, the observer state converges to the induction motor state. Such an observer will be a natural observer and its convergence will be as fast as that of the motor in reaching its steady state, which is fast enough for most applications. To achieve the convergence starting with $\hat{T}_L \neq T_L$, a new load torque estimation scheme is proposed.

The proposed scheme can be used with various induction motor models. In this paper, the following 5th order model in a dq reference frame rotating with an angular speed of ω_e is used:

$$\begin{bmatrix} \dot{i}_s \\ \dot{\psi}_r \\ \dot{\omega}_r \end{bmatrix} = \begin{bmatrix} -\left(\frac{L_r R_s + M^2/\tau_r}{\sigma L_s L_r} + j\omega_e\right) i_s + \frac{M}{\sigma L_s L_r} \left(\frac{1}{\tau_r} - j\omega_r\right) \psi_r \\ \frac{M}{\tau_r} i_s - \left(\frac{1}{\tau_r} + j(\omega_e - \omega_r)\right) \psi_r \\ \frac{3 n_p M}{2 J L_r} \text{Im}(\psi_r^* \cdot i_s) - \frac{f_d}{J} \omega_r - \frac{1}{J} T_L \end{bmatrix} + \begin{bmatrix} \frac{1}{\sigma L_s} \\ 0 \\ 0 \end{bmatrix} v_s \quad (8)$$

where $v_s = v_d + jv_q$ is the applied stator voltage, $i_s = i_d + ji_q$ is stator current, $\psi_r = \psi_d + j\psi_q$ is rotor flux, ω_r is rotor speed in electrical *rad/s*, T_L is load torque, L_r , L_s and M are rotor, stator and mutual inductances respectively, $\tau_r = L_r/R_r$ is rotor time constant, R_s and R_r are stator and rotor resistances respectively, $\sigma = (L_r L_s - M^2)/(L_s L_r)$ is the leakage constant, n_p is the number of pole pairs, J is inertia, f_d is friction constant and the superscript “*” denotes the conjugate operator. The system inputs are v_d and v_q , and the system outputs are i_d and i_q . The motor shaft speed is required for speed control. However, because speed sensorless operation is considered, estimated speed will be used for control purposes.

Assuming that the load torque is to be estimated, a natural observer for the induction motor is given by the same form as (8) with estimated quantities accompanied by hats “^”.

$$\begin{bmatrix} \dot{\hat{i}}_s \\ \dot{\hat{\psi}}_r \\ \dot{\hat{\omega}}_r \end{bmatrix} = \begin{bmatrix} -\left(\frac{L_r \hat{R}_s + M^2/\hat{\tau}_r}{\sigma L_s L_r} + j\omega_e\right) \hat{i}_s + \frac{M}{\sigma L_s L_r} \left(\frac{1}{\hat{\tau}_r} - j\hat{\omega}_r\right) \hat{\psi}_r \\ \frac{M}{\hat{\tau}_r} \hat{i}_s - \left(\frac{1}{\hat{\tau}_r} + j(\omega_e - \hat{\omega}_r)\right) \hat{\psi}_r \\ \frac{3 n_p M}{2 J L_r} \text{Im}(\hat{\psi}_r^* \cdot \hat{i}_s) - \frac{f_d}{J} \hat{\omega}_r - \frac{1}{J} \hat{T}_L \end{bmatrix} + \begin{bmatrix} \frac{1}{\sigma L_s} \\ 0 \\ 0 \end{bmatrix} v_s \quad (9)$$

A load torque estimation scheme is proposed using the active power error as the correction term. Since there is no feedback in the natural observer, (9), it is clear that the observer's power, \hat{P} , converges to a higher value than the induction motor's power, P , in the steady-state if the power consuming direction of the torque is selected as positive and the estimated load torque is higher than the actual torque. Based on this fact, a PID estimation scheme can be developed using $e_p = \hat{P} - P$ as the correcting term. However, the power consuming direction of the torque can change during operation, for example, when the speed is reversed. Therefore, changing the sign of the PID gains is crucial for the success of the adaptation scheme. The signs of the gains are determined according to the error dynamics of e_p , which are controlled by \hat{T}_L . The sign of \hat{T}_L in the error differential equation of e_p determines the sign of the gains. To establish such an error differential equation, derivatives of e_p are taken until \hat{T}_L appears

$$e_p = \hat{P} - P = v_d(\hat{i}_d - i_d) + v_q(\hat{i}_q - i_q) \quad (10)$$

$$\begin{aligned} \dot{e}_p &= v_d \dot{\hat{i}}_d + v_q \dot{\hat{i}}_q + \dots (\text{other terms}) \dots \\ &= \frac{M}{\sigma L_s L_r} (v_d \hat{\psi}_q - v_q \hat{\psi}_d) \hat{\omega}_r + \dots \end{aligned} \quad (11)$$

where “...” denotes all the other terms not including $\hat{\omega}_r$. These terms are disregarded because \hat{T}_L appears only in the derivative of $\hat{\omega}_r$. Then

$$\ddot{e}_p = -\frac{M}{\sigma L_s L_r J} (v_d \hat{\psi}_q - v_q \hat{\psi}_d) \hat{T}_L + \dots \quad (12)$$

$$e_p + \alpha_1 \dot{e}_p + \alpha_0 e_p = d - \frac{M}{\sigma L_s L_r J} (v_d \hat{\psi}_q - v_q \hat{\psi}_d) \hat{T}_L \quad (13)$$

where α_0 and α_1 are arbitrary positive constants for the desired convergence rate, $\hat{\psi}_d$ and $\hat{\psi}_q$ are the observer rotor flux estimations, v_d and v_q are input voltages, and “...” and d summarise all the other terms not including \hat{T}_L . Assuming d and $(v_d \hat{\psi}_q - v_q \hat{\psi}_d)$ change

slowly, a PID scheme will force e_p to converge to zero. If the load torque estimate \hat{T}_L is not limited, it may reach unacceptable values that may cause unstable oscillations. Therefore, \hat{T}_L is kept to within the predetermined range $[T_{\min}, T_{\max}]$. With the same inputs as the actual system, even if \hat{T}_L is incorrect, the speed estimation error will not reach excessive values if \hat{T}_L is kept within the predetermined limits. Additionally, a rate limiter can be used to prevent rapid changes in the estimated torque thereby ensuring that the state and torque estimates converge smoothly to the actual values. This adaptation scheme, which works with the natural observer (9), can be summarised as follows:

$$\hat{T}_L = K_D \dot{e}_p + K_P e_p + K_I \int e_p dt \quad \text{limiting} \quad \hat{T}_L \in [T_{\min}, T_{\max}] \quad (14)$$

$$\text{sign}(K_D) = \text{sign}(K_P) = \text{sign}(K_I) = \text{sign}(v_d \hat{\psi}_q - v_q \hat{\psi}_d) \quad (15)$$

When the gains are changing in value or sign, the integral value in (14) is re-initiated to find the same \hat{T}_L value with the new sign in order to prevent discontinuity. Denoting this integral as ξ , the re-initiation is performed as follows:

$$\xi^+ = \frac{1}{K_I^+} \left((K_D^- - K_D^+) \dot{e}_p + (K_P^- - K_P^+) e_p + K_I^- \xi^- \right) \quad (16)$$

where superscripts “ $-$ ” and “ $+$ ” denote the values just before and just after the re-initiation process respectively. Similarly, when \hat{T}_L strays outside of its predetermined limits, the integral value is re-initiated so that (14) gives the limited \hat{T}_L value.

In PID schemes, the proportional gain and particularly the derivative gain are usually selected to be very small, or they may even be omitted. The proposed adaptation scheme is still feasible even if the derivative term is omitted. Successful adaptation is not, however, guaranteed when the derivative term is omitted although both simulations and experiments

have resulted in successful estimations. Then, (9) and (14)-(16) describe a full order speed sensorless induction motor observer with load torque adaptation as shown in Figure 3.

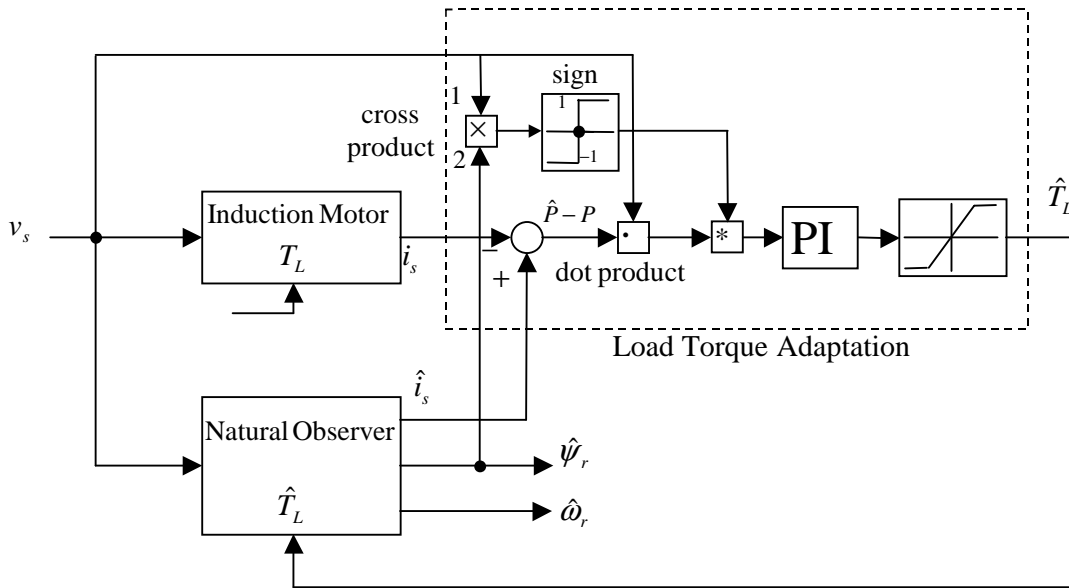


Figure 3: Natural observer for induction motor with load torque adaptation.

There are a number of techniques with torque estimation [12-18] for speed sensorless operations but they differ significantly from the technique presented here. The observer (9) with (14)-(16) is similar to that described in [17], but the methods used for speed and torque estimation are different. The speed estimation techniques in [17] and in Kubota's method [11-13] always need some error (correction) term in order to follow speed changes. This results in the estimations always lagging the actual values. In the technique proposed in this paper the speed estimation follows the speed changes simultaneously unless a sudden change occurs in the load torque. Simulation and experimental results have shown that even during sudden load torque changes the estimations converge at a fast rate. It is shown in [16] and [19] that some terms act altogether as if to produce a load torque estimation, however, the technique proposed here is considered to be simpler and more efficient.

IV. EXPERIMENTAL AND SIMULATION RESULTS

A. Simulation Results For Speed Sensorless DC Servomotor

The dc servo model (3) for $R_a = 3.2\Omega$, $L_a = 8.6mH$, $K_t = 0.017 Nm/A$, $K_b = 0.060Vs/rad$, $f_d = 0.00012Nm \cdot s/rad$ and $J = 30 \times 10^{-6} kgm^2$ has been simulated with the adaptive observer (4)-(5) and control (7), using $K_D = 0.01Vs^2/rad$, $K_p = 0.4Vs/rad$, $K_i = 4V/(rad \cdot s)$ and $\mu = -0.0003 Nm/As$. The speed reference, ω_{ref} , is $100 rad/s$ for $0 \leq t < 2s$ and $t \geq 4s$ whilst it is $-100 rad/s$ for $2s \leq t < 4s$. The control voltage, v_a , is limited between $v_{min} = -15V$ and $v_{max} = 15V$, for which the feasible torque limits at $\mp 100 rad/s$ can be calculated as $\mp 0.036 Nm$. Therefore, as a reasonable choice, \hat{T}_L is limited between $T_{min} = -0.04 Nm$ and $T_{max} = 0.04 Nm$. The actual load torque $T_L = 0.01 Nm$ for $0 \leq t < 5s$ and $T_L = 0.03 Nm$ for $t \geq 5s$. Thus, this simulation includes both speed reversal and sudden load changes as shown in Figures 4 and 5.

Figure 4 shows the speed and current together with their estimations. As is shown in the figure, convergence is achieved quickly and thereafter the error remains at zero even when the speed is reversed. As shown in Figure 5, when the load torque changes suddenly, a transient error occurs followed by the \hat{T}_L estimate tracking the actual torque quickly after the change. The load torque estimate, \hat{T}_L , tracks the actual torque quickly after the change, as shown in Figure 5. The control signal, v_a , tends to exceed its limits only at the instants when the speed reference is reversed. The new scheme proposed here is therefore a successful means of speed sensorless control of a servomotor, as shown by the simulation results.

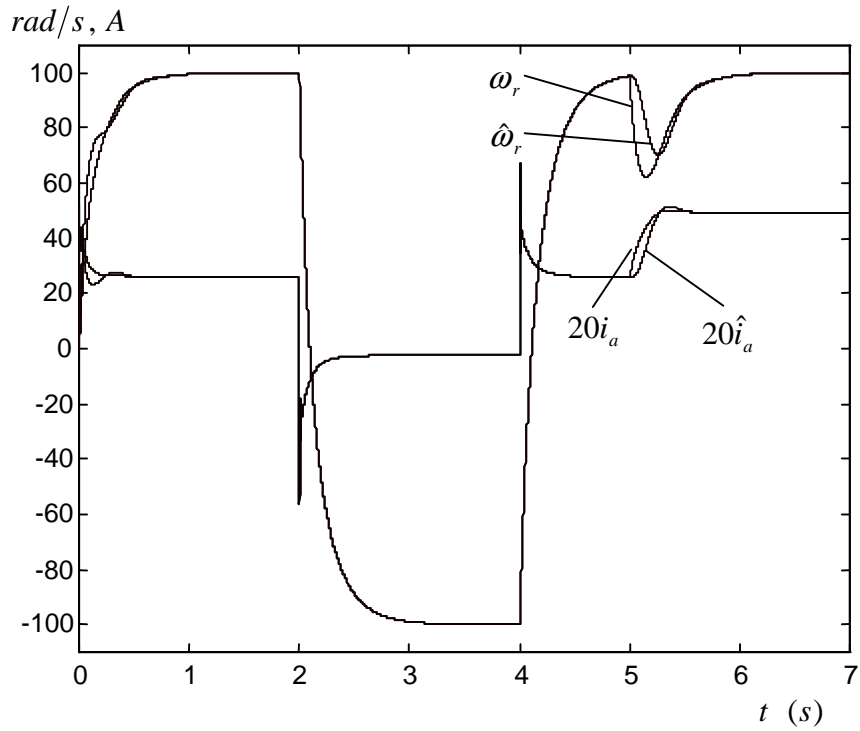


Figure 4: Convergence of the speed and armature current estimates (scaled) for the speed sensorless dc servomotor.

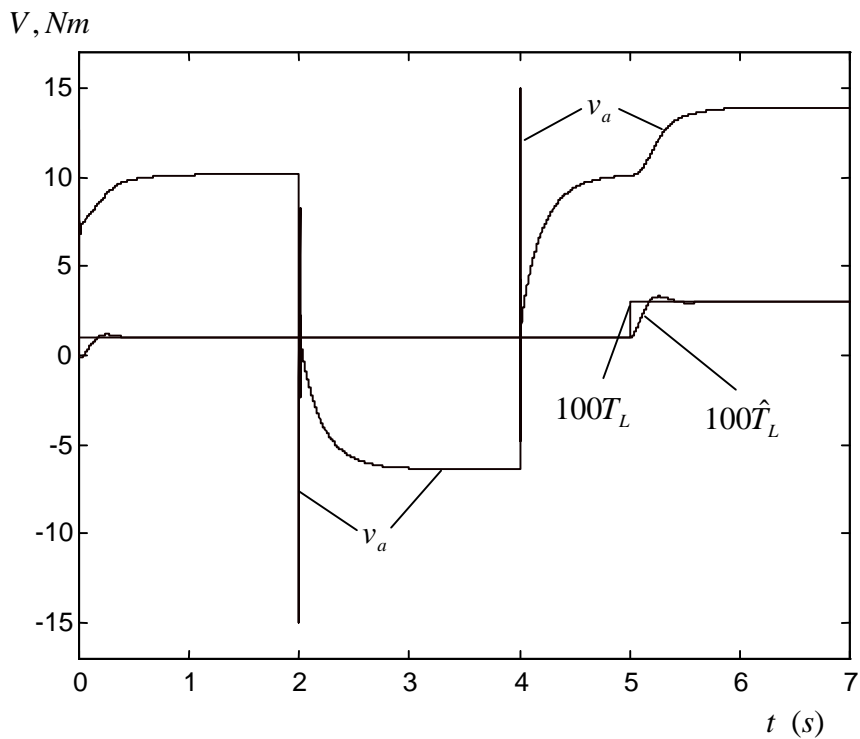


Figure 5: Armature voltage, scaled load torque and its estimation for the speed sensorless dc servomotor.

B. Experimental Results For Speed Sensorless Induction Motor

The proposed natural observer (9), with the proposed load torque adaptation scheme, has been implemented using a TMS320C30 DSP and run in parallel with a field oriented controlled induction motor. Kubota's speed adaptive observer [11], which is one of the most popular speed sensorless induction motor observers, has also been implemented using the DSP and the experimental results have been compared. The DSP runs in parallel with a commercial AC drive system that has been modified in order to isolate the speed feedback to the controller so that the drive runs as a sensorless system. The actual speed is measured for comparison purposes. The motor used in the experiments is a 3-phase, 4-pole, Δ -connected squirrel-cage induction motor. The rated values are 50Hz, 1450rpm, 440V, 11A and 5.5kW. The parameters used in the natural observer are $R_s = 1.000\Omega$, $R_r = 0.847\Omega$, $L_s = 0.13893H$, $L_r = 0.13126H$ and $M = 0.13126H$. In the experiments, an approximate induction motor equivalent circuit is used with the iron loss equivalent resistance, $R_o = 765.8\Omega$, placed in parallel with the stator voltage source. That is, the current through this resistance is calculated from the applied stator voltage and is then subtracted from the measured stator current and the resultant current is then used in the observer.

The experimental data has been acquired using a digital storage oscilloscope, which provides filtered plots. The experimental plots are presented over 32s periods to ensure clarity. The DSP programs run and communicate with the drive using 0.5ms time steps. However, at this fast scan rate the drive can provide only two measurement signal outputs. Therefore, the drive is used as a current controlled voltage source inverter. The current references are given to the drive by the DSP with a 7.5ms scan rate and the voltage references are given to the DSP by the drive with 0.5ms time steps.

The torque current is limited within $\mp 20A$ until the estimated speed enters a band of $\mp 30 \text{ rad/s}$ around the reference speed when current is then reduced to $\mp 2A$. Torque limits are $\mp 85 \text{ Nm}$ for the estimators. The magnetising current reference is kept constant at $5.72A$. Initial conditions are all zero for the observers, estimated torque and speed. In Kubota's technique, the gain matrix is selected to be zero, which is the optimal choice.

In the speed reversal test the speed reference is toggled every $8s$ between $80\pi \text{ rad/s}$ and $-80\pi \text{ rad/s}$ without a reference model. The estimated torque's slope is limited to within $\mp 10 \text{ Nm/s}$. The torque adaptation gains are $K_D = 0$, $K_p = 0.01$ and $K_I = 0.5$ for (14)-(15). Proportional and integral gains for Kubota's speed adaptation scheme [11] are selected as $0.05 \text{ rad}/(\text{VAs}^2)$ and $6 \text{ rad}/(\text{VAs}^3)$ respectively which, following a number of trials, have been shown to give optimal results. Figure 6 and Figure 7 show the experimental results for speed reversal tests and illustrate that the proposed scheme yields better results than Kubota's. The estimated and actual speeds with Kubota's method oscillate as the speed is changing, particularly around zero speed. The proposed scheme also yields better results (less oscillation and ripple) in both transient and steady states. No load is applied to the motor in this test but, because of Coulomb friction, there exists a small constant torque for each direction of rotation as can be seen in Figure 7.

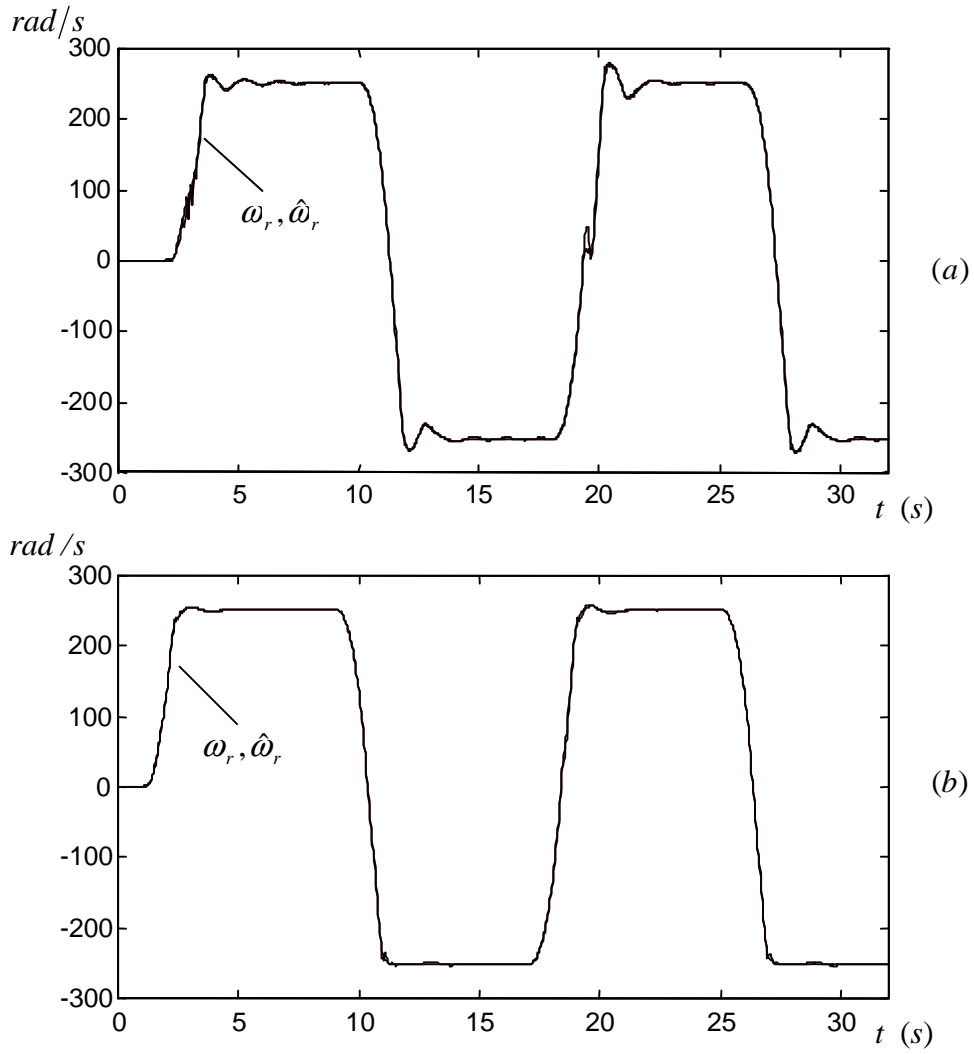


Figure 6: Speed reversal test results without any load: (a) Kubota's method. (b) Natural observer with load torque adaptation, (9) and (14)-(16).

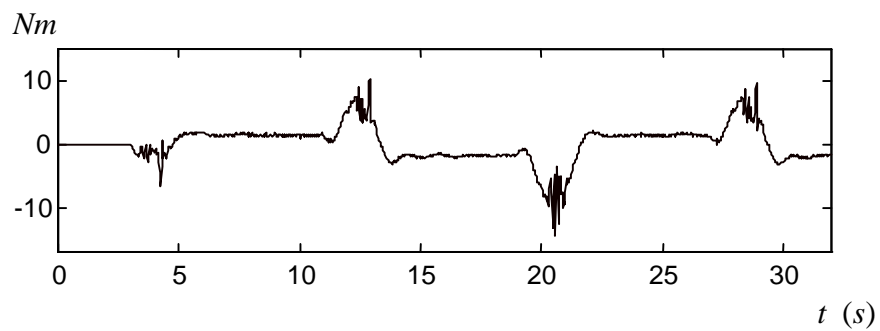


Figure 7: Load torque estimation with the proposed scheme, (9) and (14)-(16), in speed reversal test.

During sudden loading and unloading tests the speed reference is kept constant at $80\pi \text{ rad/s}$. To improve response, the torque estimation rate limit for the positive slope is increased to $+40 \text{ Nm/s}$ whilst the negative slope limit is maintained as -10 Nm/s . The integral gain of the torque estimator is also increased to $K_I = 1$ in order to obtain a quicker response. The torque current limits used in the previous test are not sufficient to drive this load at the reference speed hence the torque current limits are enlarged to $\mp 10 \text{ A}$, 4 s after start up. There is no load at start up, but a load of approximately 20 Nm is suddenly applied after the settled speed is achieved and after the speed has settled again, the load is suddenly removed. Results are shown in Figure 8 and Figure 9. The speed and estimated speed responses for the two schemes are almost the same at sudden loading, however the proposed scheme results in a much improved response (shorter rise time and fewer oscillations) at sudden unloading. This results from the fact that the proposed scheme can use different rate limits at load torque increase and decrease. The increase in the transient of the proposed scheme is due to the increase in the integral gain of the torque estimator. This can be improved if required using the previous gains at start up. Figure 10 compares the speed errors resulting from Kubota's method and from the proposed method and confirms the improvements in performance resulting from the proposed scheme.

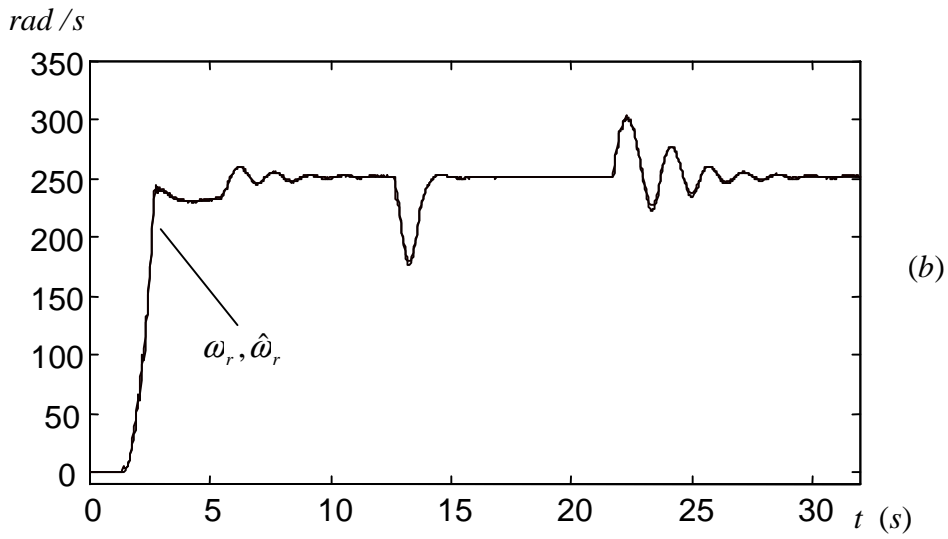
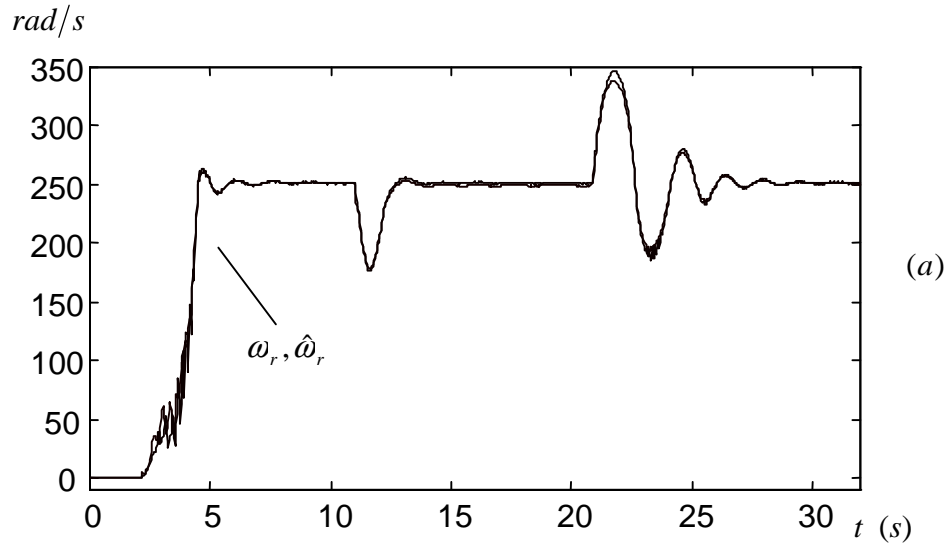


Figure 8: Estimated and actual speeds in sudden loading test: (a) Kubota's method. (b) Natural observer with load torque adaptation using active power error, (9) and (14)-(16).

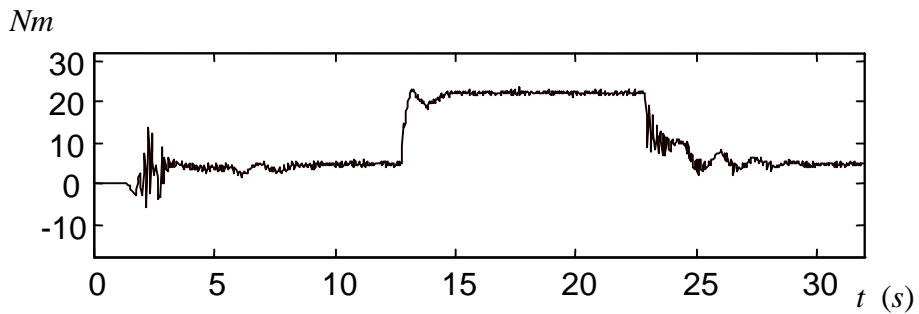


Figure 9: Load torque estimation with the proposed scheme, (9) and (14)-(16), in sudden loading test.

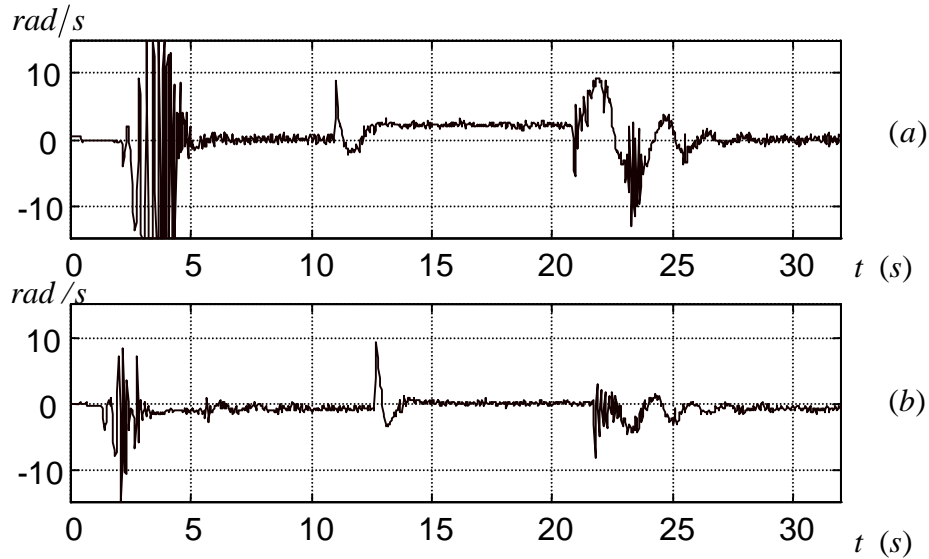


Figure 10: Speed estimation errors in sudden loading test for (a) Kubota's method. (b) Natural observer with load torque adaptation using active power error, (9) and (14)-(16).

IV. CONCLUSIONS

The natural observer design technique and adaptation algorithms have been shown to be very simple and successful. Excellent performance for dc servo and induction motor observers for speed sensorless operation has been demonstrated and verified by simulation and experiments.

Natural observers have a number of advantages over the conventional observers. In particular, since in the natural observer convergence is achieved using parameter adaptation, the convergence problems of the adaptation algorithm and observer are simplified. Also, since the feedback signal is used only in the adaptation scheme, the measurement noise is filtered by the adaptation scheme. It is also important to note that the natural observer further filters the noise without causing any delay. As a result, natural observers are therefore less sensitive to noise compared to the conventional observers using feedback. For complicated non-linear systems, conventional observers are usually designed using some approximation of

the system equations. Under certain conditions, for example when the states are changing quickly, they may not follow the actual system. However, natural observers are designed in the same form as the actual system and therefore follow the actual states very closely even when the states are changing very quickly. In addition, it is possible to smooth the convergence of the natural observers by applying amplitude and rate limiters to the parameter estimations.

Application of the proposed natural observer and adaptation methods to a wide range of bounded-input bounded-output non-linear systems will be considered in future papers.

REFERENCES

- [1] A.H. JAZWINSKI, “*Stochastic Processes and Filtering Theory*”, Academic Press, New York, 1970.
- [2] Y.R. KIM, S.K. SUL and M.H. PARK, “Speed sensorless vector control of induction motor using extended Kalman Filter”, *IEEE Trans. Industry Applicat.*, Vol. 30, No. 5, 1994, pp.1225-1233.
- [3] G.G. SOTO, E. MENDES and A. RAZEK, “Reduced-order observers for flux, rotor resistance and speed estimation for vector controlled induction motor drives using the extended Kalman filter technique”, *IEE Proc. Electr. Power Appl.*, Vol. 146, No. 3, 1999, pp.282-288.
- [4] J. BIRK and M. ZEITZ, “Extended Luenberger observer for non-linear multivariable systems”, *Int. J. Control*, Vol. 47, No. 6, 1988, pp.1823-1836.
- [5] T. DU, P. VAS and F. STRONACH, “Design and application of extended observers for joint state and parameter estimation in high-performance AC drives”, *IEE Proc. Electr. Power Appl.*, Vol. 142, No. 2, 1995, pp.71-78.
- [6] F. PROFUMO, G. GRIVA, A. TENCONI, M. ABRATE and L. FERRARIS, “Stability Analysis of Luenberger Observers for speed sensorless high performance spindle drives”, *EPE '99 Lausanne Conf. Rec.*, 1999.
- [7] S. TAMAI, H. SUGIMOTO and M. YANO, “Speed sensorless vector control of induction motor with model reference adaptive system”, *IEEE IAS Ann. Meet.*, 1987, pp.189-195.

- [8] C. SCHAUDER, "Adaptive speed identification for vector control of induction motors without rotational transducers", *IEEE Trans. Industry Applicat.*, Vol. 28, No. 5, 1992, pp.1054-1061.
- [9] F.Z. PENG and T. FUKAO, "Robust speed identification for speed sensorless vector control of induction motors", *IEEE T-IA*, Vol.30, No.5, 1994, pp.1234-1240.
- [10] H. TAJIMA and Y. HORI, "Speed sensorless field-orientation control of the induction machine", *IEEE T-IA*, Vol. 29, No. 1, 1993, pp.175-180.
- [11] H. KUBOTA, K. MATSUSE and T. NAKANO, "New adaptive flux observer of induction motor for wide speed range motor drives", *IEEE IECON '90 Conf. Rec.*, Vol. 2, 1990, pp.921-926.
- [12] H. KUBOTA and K. MATSUSE, "Robust field oriented induction motor drives based on disturbance torque estimation without rotational transducers", *IEEE IAS Conf. Rec.*, Vol. 1, 1992, pp.558-562.
- [13] H. KUBOTA and K. MATSUSE, "Speed sensorless field-oriented control of induction motor with rotor resistance adaptation", *IEEE Trans. Industry Applicat.*, Vol. 30, No. 5, 1994, pp.1219-1224.
- [14] WONHAM, "On a matrix Riccati equation of stochastic control", *SIAM J. Control*, Vol. 6, 1968, pp.681-697.
- [15] T. OHTANI, N. TAKADA and K. TANAKA, "Vector control of induction motor without shaft encoder", *IEEE Trans. Industry Applicat.*, Vol. 28, No. 1, 1992, pp.157-164.
- [16] K. OHYAMA, G.M. ASHER and M. SUMNER, "Comparison of the practical performance and operating limits of sensorless induction motor drive using a closed loop flux observer and a full order flux observer", *EPE '99 Lausanne Conf. Rec.*, 1999.
- [17] H. HOFMANN and S.R. SANDERS, "Speed-sensorless vector torque control of induction machines using two-time scale approach", *IEEE Trans. Industry Applicat.*, Vol. 34, No. 1, 1998, pp.169-177.
- [18] N. KASA and H. WATANEBE, "A torque ripples compensating technique based on disturbance observer with wavelet transform for sensorless induction motor drive", *IEEE IECON '98 Conf. Rec.*, Vol. 2, 1998, pp.580-585.
- [19] P.L. JANSEN and R.D. LORENZ, "Accuracy limitations of velocity and flux estimation in direct field oriented induction machines", *EPE '93 Brighton Conf. Rec.*, 1993, pp.312-318.